ABSOLUTE PULSED-MODE, LONG-DURATION INTEGRAL FIELD INSTRUMENTATION USING A MULTI-SENSOR APPROACH

A. Ganesh*[1], A. Bellelli[1], M. Bonora-Tam[1], M. Buzio[1], C. Petrone[1]
[1]European Organization for Nuclear Research (CERN), Geneva, Switzerland

Abstract

A recent upgrade of the CERN Super Proton Synchrotron (SPS) quadrupole magnet measuring system enables high relative accuracy on the order of 10^{-5} over cycle sequences up to 800 seconds long, as needed for machine-learning based modeling and control of hysteresis effects in the frame of the Efficient Particle Accelerator (EPA) initiative. A new fluxmeter assembly integrates multiple arrays of PCB induction coils with Hall probes and local coils for in-situ cross-calibration, while new FFMM (Flexible Framework for Magnetic Measurements) C++ classes provide automation of complex excitation current cycles, data reduction and database storage. A Python data processing pipeline uses Kalman filters to fuse multiple sensors, correcting for integrator drift. This enables absolute measurements even without traditional Nuclear Magnetic Resonance (NMR) probes, which operate only in uniform fields.

INTRODUCTION

The SPS is a fast-ramped machine with iron-dominated magnets affected by strong (~ 6%) non-linear eddy currents and magnetic hysteresis effects [1]. The bending dipole field is measured in real time by a so-called B-train system [2, 3] combining integral induction coils with NMR probes, used as a ppm-level absolute reference, installed in reference magnets in series with the ring dipole magnets. A similar system ("G-train") was attempted in the past for the main focusing (QF) and defocusing (QD) quadrupole magnets, but since NMR probes do not work at all in field gradients [1, 4], the accuracy was too low. Alternative, recent approaches shift the burden from real-time setups onto neural-network field-prediction models trained on data obtained from extensive measurement campaigns, carried out in the laboratory under more favourable, controlled conditions [5–7]. Hysteresis model training relies crucially on the ability to measure the integral field at a 10^{-5} relative accuracy level over many, several minutes-long sequences of cycles in different combinations, without interruption. The legacy integral induction coils were designed to compare magnets against reference units in differential mode over current pulses lasting only a few seconds, and are inadequate for longer durations. This paper presents the new multi-sensor quadrupole fluxmeter developed to meet this demand. We describe in detail the instrumentation setup and compare classic piecewise linear integrator drift correction with a novel sensor fusion method, providing result examples and conclusions.

* abhishek.ganesh@cern.ch

MEASUREMENT SETUP

Magnet and Operational Cycles The 3050 mm-long SPS QF/QD quadrupole magnets reach 21.7 T/m at 2110 A, well into the saturated regime of the iron. Their 1260 A RMS rating caps the current that can be sustained continuously, and with it the upper bound of any DC field characterization. Classical instruments such as rotating coils or stretched wires deliver the highest absolute accuracy but require steady-state excitation. Excitation current is supplied by a 6 kA peak / 3.2 kA RMS Holec power converter, voltage-driven by a 24-bit DAC source providing a nominal 7.775 mA resolution and read by a DCCT with 1.3 A accuracy. The two supercycles (series of consecutive acceleration cycles) used for the tests reported here are the LHC2/SFTPRO/MD1 (Q20 beam optics) and LHCPILOT/SFTPRO/MD1 (Q26 beam optics) cycles. The tests included 70 consecutive cycles lasting up to 800 s, with plateaus at flat-bottom (55 A), injection (200 A) and extraction (2110 A).

Fluxmeter Assembly The fluxmeter (Fig. 1(a)) is comprised of $7 \times (600.0 \pm 0.2)$ mm-long, 136.0 ± 0.2 mm wide 12-layer coil array PCBs, covering the whole extension of the magnet's field and mounted on a 3D-printed Poly-lactic Acid (PLA) support structure shaped to fit the quadrupole bore with or without vacuum chamber. One array of hybrid Hall-probe/induction coil sensors (Fig. 1(b)) is installed on the PCB at the centre of the magnet.

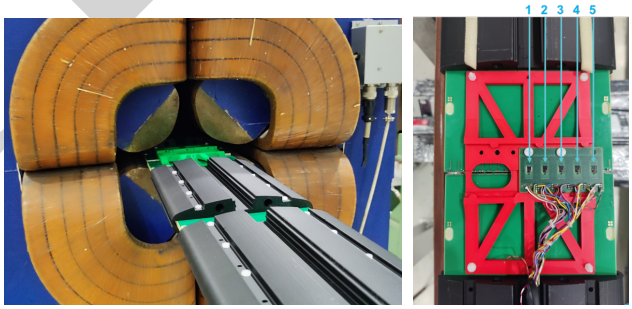

(a) Multi-sensor fluxmeter assembly inside the SPS quadrupole bore.

(b) Hall probe array with short coils.

Figure 1: Fluxmeter assembly.

Induction coil array Each PCB carries 21 parallel 596.0 mm-long, 4.92 mm wide, 84-turn induction coils, spaced $\Delta x = 6.4$ mm apart, with surfaces individually calibrated against NMR in a reference dipole averaging $A = 0.1086\,\mathrm{m}^2$ with $\sigma_A/A = 1.0 \times 10^{-5}$. Any pair of coils can in principle be connected in series opposition (known as *bucking*) to directly provide the field gradient G suppressing the dipole component and common-mode pickup [8].

In our present implementation, the corresponding coils in all PCBs are first connected in series, giving an effective $A_{\mathrm{eff}} = 0.7607\ \mathrm{m}^2$, and then subtracted pairwise to obtain $N_{\mathrm{p}} = 10$ adjacent integral gradient coil pairs (index p), each linked with the flux $\Phi_{p,p+1} = GA_{\mathrm{eff}}\Delta x$.

Hybrid Hall probe/small coil array Five Hall probes (index h) with transversal spacing $d = 12$ mm (Fig. 1b) are included to capture the absolute field gradient, ideally providing the needed integration constant for the fluxmeter. Each probe was calibrated against NMR in a reference dipole according to a quadratic model. $B_h(V) = a_{2,h}V^2 + a_{1,h}V + a_{0,h}$. The pairwise gradient $(B_{h+1} - B_h)/d$ is averaged over four pairs to yield the central Hall gradient G_{H}. The ratio between the integral and local gradient, i.e. the magnetic length L_{m}, depends upon the shape of the longitudinal field profile, which is affected by saturation and eddy currents. Related errors up to ~ 3% can be avoided by using the measured local gradient only under low-field, static conditions, such as achieved on a cycle flat-bottom. In addition, a small induction coil was wound around each Hall probe and calibrated against NMR in a reference dipole, to provide an in-situ gain calibration cross-check. Assuming near-perfect linearity of the coil, the ratio $\kappa_h = \Delta B_{\mathrm{coil}}/\Delta B_{\mathrm{Hall}}$ can be computed between any two consecutive stable plateaus to correct any change of Hall gain with respect to the initial calibration. However, this method does not apply to the offset term a_0, due to thermal effects and 1/f noise, and remains a significant source of error.

ACQUISITION AND POST-PROCESSING

FFMM-controlled Data Acquisition The FFMM framework [9] is used to synthesize the excitation current waveform with 1 ms resolution, trigger the synchronous acquisition of the 21 input signals (ten gradient coil-pair voltages, five Hall voltages, five local coil voltages, and the DCCT) by a 20-bit Σ-Δ ADC at $f_{\mathrm{s}} = 500$ kS/s, and store all data in HDF5 format with access to the CERN database infrastructure [10]. All coil voltages are integrated on-the-fly and converted into flux increments at 1 kHz, providing a 500-fold reduction in storage which is essential for long measurements. Raw Hall and DCCT voltages are filtered with a fourth-order, zero-phase, Butterworth low-pass filter (500 Hz cut-off, optional 50 ms median kernel) and downsampled to 1 kHz to match the flux measurement.

Piecewise Linear Drift Correction Flux integration is affected by an additive voltage offset V_d due to $1/f$ noise, leading to unbounded, fluctuating drift [11]. For classic piecewise linear correction, the acquisition is first split automatically into cycles (index j) at anchors set at the midpoint t_j of flat-bottom plateaus, identified using the reference current I_{ref} where $50 \le I_{\mathrm{ref}} \le 58$ A and $|dI_{\mathrm{ref}}/dt| < 10^{-6}$ A/s for ≥ 4 s. At every anchor, the offset of each gradient coil signal $\hat{V}_{d,p}(t_j)$ is estimated as the average over a supposed zero-signal 0.2 s window, defined after any eddy-current decay transient. The offset-corrected voltage $(V_p(t) - \hat{V}_{d,p}(t_j))$ is then integrated, resulting in a feed-forward drift-corrected flux $\Phi_p(t)$ [12]. The integrated gradient is given by:

$$G d\ell_p(t) = \frac{\Phi_p(t)}{A_{\mathrm{eff},p}\,\Delta x}\, L_{\mathrm{eff},p} \tag{1}$$

where the effective total coil length $L_{\mathrm{eff},p}$ is corrected to account for the the 4-mm longitudinal gap between PCBs, and then averaged over the ten gradient coils to obtain $Gd\ell(t)$.

Magnetic Length The magnetic length $L_{\mathrm{m}} = 3007 \pm 86$ mm is obtained from the ratio of integrated and local gradient on the injection plateau. The uncertainty is the quadratic combination of measurement reproducibility (4.6 mm) and scatter of the averaged gradients (86 mm).

Absolute Referencing As the piecewise drift correction resets the integrated flux to zero at the beginning of each cycle, the absolute gradient was recovered by adding the extrapolated Hall gradient to each cycle, and then removing any residual discontinuity δ_j by an additional linear correction:

$$G d\ell_{\mathrm{abs}}(t) = \underbrace{G d\ell(t)}_{\text{coils, Eq. (1)}} + \underbrace{\bar{G}_{\mathrm{H}}(t_j)\, L_{\mathrm{m}}}_{\text{extrapolated gradient}} - \underbrace{\delta_j \frac{t - t_j}{t_{j+1} - t_j}}_{\text{residual correction}} \tag{2}$$

for $t \in [t_j, t_{j+1})$, where $\bar{G}_{\mathrm{H}}(t_j)$ is the Hall integral gradient averaged over a 100 ms window at anchor t_j, and the per-cycle drift residual is $\delta_j = G d\ell_j(t_j) - G d\ell_{j-1}(t_j)$.

MEASUREMENT RESULTS

Absolute Integral Gradient and Hysteresis Figure 2 shows $Gd\ell_{\mathrm{abs}}$ for 70 consecutive machine cycles. When the supercycle simply repeats, the SFTPRO flat-top gradient is reproducible within 18 ppm over a subset of 29 stable cycles (after initial accommodation). When an LHCPILOT cycle is inserted between SFTPRO and MD1 in Q26 mode, the SFTPRO flat-top gradient shifts by 0.0435 T m/m (718 ppm) in Fig. 3, well above the cycle-to-cycle noise floor. This value is computed over the flat-top window indicated by the black rectangle in Fig. 2 ($Gd\ell_{\mathrm{abs}} \in [59, 62]$ T m/m). The minimum detection threshold for hysteresis-driven gradient change is 1.15 mT m/m (26 ppm).

Uncertainty Budget Equation (2) makes the two accuracy regimes explicit. The *absolute* integral gradient depends on the full multiplicative chain of equation 1 plus the Hall calibration and L_{m} from the anchoring term. The *relative* gradient (hysteresis loops, cycle-to-cycle differences) cancels all constant geometric and calibration factors, leaving only flux integration noise.

The absolute scale is overwhelmingly dominated by L_{m}, which may be attributed essentially to uncorrected Hall probe offsets. Relative measurements are two orders of magnitude better; random integration errors after piecewise correction are as low as 17 ppm, whereas systematic (i.e. potentially amenable to further calibration) geometry-related errors remain in the range of a few hundred ppm.

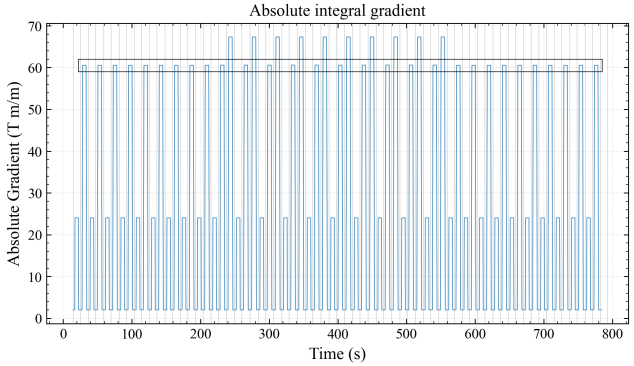

Figure 2: $Gd\ell_{\mathrm{abs}}$ for 70 consecutive cycles with the LHCPILOT/SFTPRO/MD1 (Q26) supercycle. Black rectangle: SFTPRO flat-top windows used for hysteresis analysis.

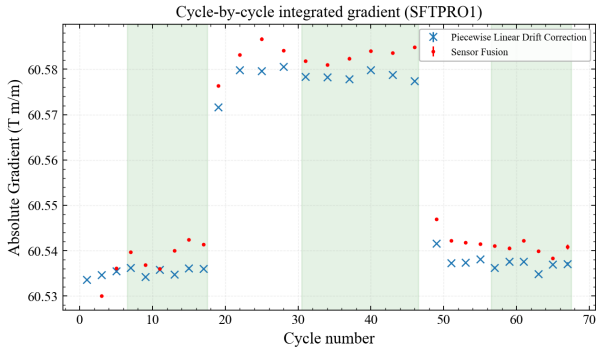

Figure 3: Cycle-by-cycle SFTPRO flat-top gradient with marked green regions representing stable cycles.

Table 1: Uncertainties for Integral Gradient Measurement

Source	$Gd\ell$ **[ppm]**
Effective coil area A_{eff}	841
Geometry L_{eff}, Δx	~500
Hall calibration (+in-situ κ_h)	~100
Magnetic length L_{m}	28 700
Integrator drift (uncorrected)	130
Integrator drift (piecewise corr.)	17
Integrator drift (sensor fusion)	14
Total (RMS)	≈ 28 700

MULTI-SENSOR FUSION

As an alternative drift correction method, we turn to sensor fusion techniques to address the major weakness of the piecewise correction, i.e. the fluctuation of drift error in between anchor points [11]. We have tested a causal Kalman filter at 1 kHz, in which the Hall and coil measurements are combined and the voltage offset of every coil pair is promoted to a separate variable in the state vector $\mathbf{x}_k = [Gd\ell_k, V_{d,k}^{(1)}, \ldots, V_{d,k}^{(N_p)}]^\top$, evolving as an independent random walk $V_{d,k}^{(p)} = V_{d,k-1}^{(p)} + w_{V,k}^{(p)}$. The prediction debiases each coil voltage $V_k^{(p)}$ with its own tracked drift and averages over the array.

$$Gd\ell_k^- = Gd\ell_{k-1} + \frac{T_s}{N_p}\sum_{p=1}^{N_p} c_p(V_{d,k-1}^{(p)} - v_k^{(p)}) + w_{G,k}. \quad (3)$$

where we use standard Kalman filter notation, $c_p \equiv L_{\mathrm{eff}}/A_{\mathrm{eff},p}\Delta x$ and $T_{\mathrm{s}} = 1$ ms. The Hall array provides an average scalar measurement of the central gradient:

$$z_k = Gd\ell_k + q_k. \quad (4)$$

The Hall innovation z_k is gated to a trimmed window on the injection plateau, where the Hall calibration is most accurate and eddy-current transients are absent. Outside this window the filter runs in pure prediction mode, while inside a quadratic model for the measurement variance, such as $R_k = R_0 + \gamma(dI/dt)_k^2$, restricts the contribution of the measurement to only the stable part of the cycle plateau.

All key aspects of the piecewise correction method map onto one element of the recursion: the per-cycle, per-coil pair offset estimate $\hat{V}_d^{(p)}(t_j)$ becomes the continuously tracked state $V_{d,k}^{(p)}$, the Hall-measured gradient injection at anchor points becomes a sample-wise innovation inside the allowed window, and the final linear correction step is no longer needed since no end-of-cycle discontinuity accumulates. As the effective integration time collapses to T_s, the uncertainty contribution in Table 1 of the drift further improves to 14 ppm.

CONCLUSIONS AND OUTLOOK

A novel prototype multi-sensor fluxmeter including ten differential PCB integral gradient coil pairs with five central combined Hall probes/induction coils for in-situ cross-calibration has been developed and tested on a SPS main quadrupole. We demonstrated dynamic, integrated, gradient measurements with piecewise linear drift correction over durations of more than 10 minutes with a relative uncertainty as low as 17 ppm, as required by emergent machine-learning applications [5–7, 13]. We developed a sensor fusion-based correction method with even better performance, which crucially allows adjustment at millisecond, rather than whole cycle, intervals. This method does not require stable plateaus, so it can be applied to arbitrary waveforms, and the duration of the integration can, in principle, be extended indefinitely.

Using the Hall probe array as a reference, the other major innovation of this fluxmeter is to provide the absolute integrated gradient, as needed for precise assessment of magnetic hysteresis effect in the frame of the EPA project. At this stage, however, absolute accuracy is severely limited, mainly by the uncertainty of the Hall probe offsets. We plan to reduce this drastically by implementing in-situ calibration techniques such as the spinning current method, and to further reduce the geometric systematic errors of the whole assembly by means of DC stretched-wire cross-calibration [14, 15].

REFERENCES

[1] S. Russenschuck, *Field computation for accelerator magnets*. Weinheim: Wiley-VCH, 2010. doi:10.1002/9783527635467

[2] J. Vella Wallbank *et al.*, "Development of a real-time magnetic field measurement system for synchrotron control", *Electronics*, vol. 10, no. 17, p. 2140, 2021. doi:10.3390/electronics10172140

[3] M. Buzio *et al.*, "Development of Upgraded Magnetic Instrumentation for CERN Real-Time Reference Field Measurement Systems", in *Proc. 1st Int. Particle Accelerator Conf. (IPAC'10)*, pp. 310–312, 2010.

[4] C. Grech, R. Avramidou, A. Beaumont, M. Buzio, N. Sammut, and J. Tinembart, "Metrological characterization of nuclear magnetic resonance markers for real-time field control of the CERN ELENA ring dipoles", *IEEE Sens. J.*, vol. 18, no. 14, pp. 5826–5833, 2018. doi:10.1109/JSEN.2018.2842710

[5] A. Lu, V. Kain, C. Petrone, V. Di Capua, M. Taupadel, and M. Schenk, "First operational experience with data-driven hysteresis compensation for the main dipole magnets of the CERN SPS", in *Proc. 15th Int. Particle Accelerator Conf. (IPAC'24)*, 2024. doi:10.18429/JACoW-IPAC2024-MOPS66

[6] A. Lu *et al.*, "Data-driven hysteresis compensation in the CERN SPS main magnets", in *Proc. 16th Int. Particle Accelerator Conf. (IPAC'25)*, pp. 1674–1677, 2025. doi:10.18429/JACoW-IPAC2025-WEAN2

[7] M. Amodeo, P. Arpaia, M. Buzio, V. Di Capua, and F. Donnarumma, "Hysteresis modeling in iron-dominated magnets based on a multi-layered NARX neural network approach", *Int. J. Neural Syst.*, vol. 31, no. 7, p. 2150033, 2021. doi:10.1142/S0129065721500337

[8] P. Rogacki, "A contribution to the development and characterization of rotating-coil magnetometers", Ph.D. thesis, RWTH Aachen University, 2024. doi:10.18154/RWTH-2022-03586

[9] P. Arpaia *et al.*, "A software framework for flexible magnetic measurements at CERN", in *Proc. IEEE Instrumentation and Measurement Technology Conf. (IMTC 2007)*, pp. 1–4, 2007. doi:10.1109/IMTC.2007.379293

[10] V. Inglese, "A flexible framework for magnetic measurements", Master's thesis, Università Degli Studi di Napoli Federico II, 2009. https://repository.cern/records/vb3rd-gzx62

[11] P. Arpaia, M. Buzio, V. Di Capua, S. Grassini, M. Parvis, and M. Pentella, "Drift-free integration in inductive magnetic field measurements achieved by Kalman filtering", *Sensors*, vol. 22, no. 1, p. 182, 2022. doi:10.3390/s22010182

[12] M. Amodeo, P. Arpaia, and M. Buzio, "Integrator drift compensation of magnetic flux transducers by feed-forward correction", *Sensors*, vol. 19, no. 24, p. 5455, 2019. doi:10.3390/s19245455

[13] C. Grech, M. Buzio, M. Pentella, and N. Sammut, "Dynamic ferromagnetic hysteresis modelling using a Preisach-recurrent neural network model", *Materials*, vol. 13, no. 11, p. 2561, 2020. doi:10.3390/ma13112561

[14] J. Vella Wallbank, M. Buzio, A. Parrella, C. Petrone, and N. Sammut, "Pulsed-mode magnetic field measurements with a single stretched wire system", *Sensors*, vol. 24, no. 14, p. 4610, 2024. doi:10.3390/s24144610

[15] P. Arpaia, M. Buzio, C. Petrone, S. Russenschuck, and L. Walckiers, "Multipole correction of stretched-wire measurements of field-gradients in quadrupole accelerator magnets", *J. Instrum.*, vol. 8, P06002, 2013. doi:10.1088/1748-0221/8/08/P08010